

## Brown pigment of the nanopowder spinel ferrite prepared by combustion reaction

A.C.F.M. Costa<sup>a</sup>, A.M.D. Leite<sup>a</sup>, H.S. Ferreira<sup>a</sup>, R.H.G.A. Kiminami<sup>b,\*</sup>, S. Cava<sup>c</sup>, L. Gama<sup>a</sup>

<sup>a</sup> Department of Materials Engineering, Federal University of Campina Grande, Av. Aprígio Veloso, 882, 58970-000 Campina Grande, PB, Brazil

<sup>b</sup> Department of Materials Engineering, Federal University of São Carlos, Rod. Washington Luiz, Km 235, 13565-905 São Carlos, SP, Brazil

<sup>c</sup> Interdisciplinary Laboratory of Ceramic Materials, State University of Ponta Grossa, Av. Gal. Carlos Cavalcanti, 4748, Campus Uvaranas, 84035-900 Ponta Grossa, PR, Brazil

Received 4 August 2007; received in revised form 5 December 2007; accepted 20 December 2007

Available online 18 April 2008

### Abstract

The purpose of the present work was to prepare nanometric brown pigments spinel  $(\text{Zn}_{1-x}\text{Ni}_x)\text{Fe}_2\text{O}_4$  (with  $x = 0, 0.5$  and  $1$  mol of the  $\text{Ni}^{2+}$ ) structures by combustion reaction and characterize the resulting powders. The compositions were prepared by a single-step solution combustion reaction using nitrates and urea as fuel. Stoichiometric compositions of metal nitrate and urea were calculated using the total oxidizing and reducing valences of the components, which serve as the numerical coefficients for the stoichiometric balance, so that the equivalence ratio  $\Phi_c$  is equal to unity and the energy released was maximum. The resulting powders were characterized by X-ray diffraction (XRD), nitrogen adsorption by BET, scanning electron microscopy (SEM), helium pycnometry, sedimentation, transmission electron microscopy (TEM), and CIE- $L^*a^*b^*$  color-measurements. The results demonstrated that the synthesis by combustion reaction was very fast and safe resulting in crystalline spinel containing nanoparticles (18–26 nm) for all of the compositions studied. The results demonstrate the viability of using these powders as brown ceramic pigments.

© 2008 Published by Elsevier Ltd.

**Keywords:** Combustion reaction; Nanopowders; Pigments;  $(\text{Zn}, \text{Ni})\text{Fe}_2\text{O}_4$

### 1. Introduction

Composite oxides with spinel structures ( $\text{AB}_2\text{O}_4$ ) and space group  $Fd\bar{3}m$  are important inorganic metalloid materials and are widely used in different fields. They are used not only as heat-resistant pigments, which can be applied to porcelain and ceramics,<sup>1</sup> but also as gas-sensitive materials,<sup>2</sup> catalytic materials,<sup>3</sup> magnetic materials<sup>4</sup> and wave absorption materials.<sup>5</sup>

The ferrites ( $\text{MFe}_2\text{O}_4$ ) with spinel structure involve two sites, crystallographically distinct, the tetrahedral A site and octahedral B site. They can be divided into two parts according to the arrangement of the present metal-ions between A and B sites: normal spinel  $[\text{M}^{2+}]^{\text{A}}[\text{Fe}^{3+}\text{Fe}^{3+}]^{\text{B}}\text{O}_4$  and inverse spinel  $[\text{Fe}^{3+}]^{\text{A}}[\text{M}^{2+}\text{Fe}^{3+}]^{\text{B}}\text{O}_4$ , where  $\text{M}^{2+}$  is a divalent metal-ion. It is known that Ni-ferrite is of the spinel structure, where Ni ions prefer B sites and the chemical formula can be written as  $[\text{Fe}^{3+}]^{\text{A}}[\text{Ni}^{2+}\text{Fe}^{3+}]^{\text{B}}\text{O}_4$ .<sup>6</sup> In zinc ferrite, the  $\text{Zn}^{2+}$  and  $\text{Fe}^{3+}$  ions can be

distributed over the A and B sites, and therefore, the formula is sometimes represented by  $[\text{Zn}^{2+}]^{\text{A}}[\text{Fe}^{3+}]^{\text{B}}$ .<sup>7,8</sup> For mixed ferrites ( $\text{Ni}_{0.5}\text{Zn}_{0.5}\text{Fe}_2\text{O}_4$  for example), which have typical structure of inverse spinel, the A site is occupied by ions  $\text{Zn}^{2+}$  and  $\text{Fe}^{3+}$ , while the B site is occupied by ions  $\text{Ni}^{2+}$  and  $\text{Fe}^{3+}$ . The chemical formula is represented by  $[\text{Zn}^{2+}\text{Fe}^{3+}]^{\text{A}}[\text{Ni}^{2+}\text{Fe}^{3+}]^{\text{B}}$ . The preference of the  $\text{Ni}^{2+}$  and  $\text{Zn}^{2+}$  ions by the octahedral B and tetrahedral A sites, respectively, has been demonstrated in the literature based on the preference energies for some divalent and trivalent ions in the spinel structure.<sup>9,10</sup>

Pigments are finely ground solids dispersed in a liquid for application as coatings, such as paints and inks, or for blending with other materials such as ceramics, glaze, cosmetics, and plastics. On the other hand, aqueous solutions of dyes are used for coloring paper, leather, textiles and other materials.<sup>11</sup> In the ceramic industry, many natural and synthetic pigments find practical application as coloring agents in glasses, enamels and unglazed bodies. Currently, synthetic ceramic inorganic pigments are prepared and are widely used, in particular, for the production of colored traditional glazed and unglazed tiles. When inorganic pigments are used for colored ceramic prod-

\* Corresponding author.

E-mail address: [ruth@power.ufscar.br](mailto:ruth@power.ufscar.br) (R.H.G.A. Kiminami).

ucts, certain conditions are required and in particular the pigment must be thermally stable at the firing temperature and toward the action of molten glasses (frits and/or sintering aids).<sup>12,13</sup>

The conventional preparation method of spinel pigments is the solid phase synthesis method under high temperature. The limitation of this method is that it requires a higher calcination temperature (1200 °C), which consumes a considerable amount of energy. In addition, not only is the diameter of pigments obtained large, but also the grain size distribution is nonuniform, and the pigment particle is hard, which influences the performance of pigments.<sup>14</sup>

Wide ranges of chemical methods have recently been used to obtain spinel oxides type  $MFe_2O_4$ .<sup>2,15</sup> The synthesis of spinel oxides powders using combustion reaction, which provides good compositional control, is an alternative (worth pursuing). Like some other methods that have been proposed and used to prepare ceramic powders, the combustion synthesis route enables synthesis at relatively low temperatures, and the final products are in a finely divided state with higher surface areas. The combustion synthesis offers some advantages such as the simplicity of the experimental set-up, the surprisingly short time between the preparation of the reactants and the availability of the final product, saving external energy consumption and the equally important potential of simplifying the processing prior to its forming, providing a simple alternative to other elaborate techniques.<sup>16,17</sup>

In this context, the goal of this paper is to prepare nanometric brown pigments with spinel ( $Zn_{1-x}Ni_x$ ) $Fe_2O_4$  (with  $x=0, 0.5$  and 1 mol of the  $Ni^{2+}$ ) structures by combustion reaction.

## 2. Experimental

The materials used were iron nitrate [ $Fe(NO_3)_3 \cdot 9H_2O$ ], zinc nitrate [ $Zn(NO_3)_2 \cdot 6H_2O$ ], nickel nitrate [ $Ni(NO_3)_2 \cdot 6H_2O$ ], and urea [ $CO(NH_2)_2$ ]. Stoichiometric composition of the metal nitrate and urea were calculated using the total oxidizing and reducing valences of the components, which serve as the numerical coefficients for the stoichiometric balance, so that the equivalence ratio,  $\Phi_c$ , is equal to unity and the energy released is a maximum.<sup>18</sup> Using the concepts in propellant chemistry the elements Ni, Zn, Fe, C, and H are considered as reducing elements with the corresponding valencies +2, +2, +3, +4 and +1, respectively. The element oxygen is considered as an oxidizing element with the valence -2. The valence considered for nitrogen was 0, because it is inert. The reagent mixture was placed in a vitreous silica basin; it was homogenized and heated on a hot plate at 480 °C until it self-ignited, producing typical spinels oxides. According to the valence of the reducers and oxidizer agents, the stoichiometry of the reaction for  $\Phi_c = 1$  for all of the compositions studied was calculated. The combustion reaction condition was pre-established in previously published works.<sup>16</sup> The ignition temperature was determined by an infrared pyrometer Raytek, model RAYR3I ( $\pm 2$  °C) and the ignition flame time was measured using a Condor digital chronometer. The powders were designed for NF ( $x=0$  mol of the Zn), NZF ( $x=0.5$  mol of the Zn), and ZF ( $x=1$  mol of the Zn).

These powders were characterized by X-ray diffraction (Kristalloflex D5000, Cu  $\alpha$  with a Ni filter, and scanning rate of 2°  $2\theta$ /min, in a  $2\theta$  range of 20–60°). The average crystallite sizes calculated from X-ray line broadening ( $d_{311}$ ) using Scherrer's formula<sup>19</sup> and the lattice parameters were estimated from DICVOL9 routine for Windows, using the Full-Proff software<sup>20</sup> by using Vegard's law to cations mixture from the X-ray diffraction patterns. The specific surface area was determined in  $N_2$  gas with a Quantasorb Quantachrome (model Gemini-2370 Micromeritics) apparatus. The average particle size was calculated from BET data using the equation  $D_{BET} = 6/(D_t S_{BET})$ ,<sup>21</sup> where  $D_{BET}$  = equivalent spherical diameter (nm);  $D_t$  = theoretical density ( $g/cm^3$ ) and  $S_{BET}$  = superficial area ( $m^2/g$ ). The powder density was measured using a helium pycnometer (Pycnometer Micromeritics, ACCUPYC 1330). The morphology and the size of the particles were determined by scanning electron microscopy (Philips XL30 FEG) and transmission electron microscopy (TEM). For the TEM studies, the powders were supported on carbon-coated copper TEM grids and analyzed using a Philips EM420 transmission electron microscope at an accelerating voltage of 120 kV. Bright-field and dark-field imaging was performed to reveal the size and morphology of the nanopowders. Ultraviolet radiation spectroscopy in the visible–ultraviolet light region (UV–vis spectroscopy) was performed with a Cary 100 spectrometer in the range between 350 and 750 nm for the determination of the diffuse reflectance of the obtained powders as pigments. In addition, the  $L^*a^*b^*$  color parameters of the heat-treated powders were measured using the standard lighting D65, according to the CIE- $L^*a^*b^*$  colorimetric method recommended by the CIE (Commission Internationale de l'Éclairage).<sup>17</sup> In this method,  $L^*$  is the lightness axis [black (0) → white (100)],  $a^*$  is the green (–) → red (+) axis and  $b^*$  is the blue (–) → yellow (+) axis.

## 3. Results

The combustion flame time and temperature of the combustion reaction synthesis exert an important effect on the final characteristics of the powders. These parameters depend mainly on the intrinsic characteristics of each system. For the systems ZF, NZF, and NF, the experimental values of combustion flame time and temperature of reaction obtained during the synthesis were 7.0 s and 673 °C ( $\pm 2$  °C), 12.0 s and 703 °C ( $\pm 2$  °C) and 11.0 s and 622 °C ( $\pm 2$  °C), respectively. This shows that the system NF led to a lower combustion temperature, avoiding, this way, the pre-sintering and/or the growth of particles.

The combustion flame temperature reduction and the combustion flame time small increase observed with the increase of the  $Ni^{2+}$  concentration in the redox mixture can be attributed the fiercest heat of formation of the nickel nitrate ( $\Delta H_f^\circ = -528.60$  kcal/mol) compared to the heat of formation of the zinc nitrate ( $\Delta H_f^\circ = -551.30$  kcal/mol).<sup>18</sup> Moreover, the combustion flame time and temperature are important parameters that control the phase transformation in the synthesis process by combustion reaction. The optimum temperature and time conditions vary from material to material and are determined by intrinsic characteristics of each system.

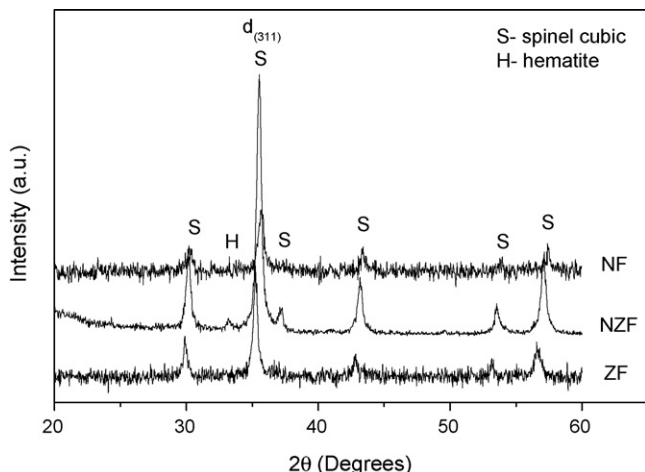


Fig. 1. X-ray diffractogram patterns of ZF, NZF, and NF powder as-prepared by combustion reaction.

The X-ray diffraction patterns of the ZF, NZF, and NF nanopowders after synthesis are shown in Fig. 1. The XRD pattern for all powders revealed the phase cubic spinel ferrite as the major phase and a small amount of hematite ( $\alpha\text{-Fe}_2\text{O}_3$ ) as the secondary phase, only for the equivalent concentration of  $\text{Ni}^{2+}$  of 0.5 mol (NZF). Considerable line broadening observed in all X-ray patterns of the spinel ferrite powders indicated the nanosized particle prepared by combustion reaction. The crystallite sizes calculated from X-ray line  $d_{(311)}$  broadening were 22; 22.2; and 18 nm for ZF, NZF and NF powders, respectively. It could also be observed that X-ray diffraction patterns  $\text{Ni}_{0.5}\text{Zn}_{0.5}\text{Fe}_2\text{O}_4$  (NZF) ferrite show characteristic peaks with larger intensity indicating, thus, a larger crystallinity when compared with the peaks observed in X-ray diffract patterns of the  $\text{ZnFe}_2\text{O}_4$  (ZF) and  $\text{NiFe}_2\text{O}_4$  (NF) ferrites powders. This can be explained by the largest combustion temperature reached during the synthesis (703 °C), which supplies larger motion force for the formation of the phase with larger crystallinity. Peaks dislocation was observed according to the increase of the introduction of the  $\text{Ni}^{2+}$  ions substituting for the ions  $\text{Zn}^{2+}$ . This occurs due to the ionic radius input difference of these ions. The ionic radius of the  $\text{Ni}^{2+}$  ion is 0.069 nm, while the ionic radius of the  $\text{Zn}^{2+}$  ion (0.074 nm) is 6.7% greater than the  $\text{Ni}^{2+}$  ion.<sup>21</sup>

Table 1 shows the characteristics of the ZF ( $\text{ZnFe}_2\text{O}_4$ ), NZF ( $\text{Ni}_{0.5}\text{Zn}_{0.5}\text{Fe}_2\text{O}_4$ ), and NF ( $\text{NiFe}_2\text{O}_4$ ) powder (specific sur-

Table 1

Powder characteristics the of pigments	ZF ( $x=1$ )	NZF ( $x=0.5$ )	NF ( $x=0$ )
Specific superficial area (BET) ( $\text{m}^2/\text{g}$ )	37.9	43.5	55.2
Particle size <sup>a</sup> (nm)	36.0	26.2	20.2
Crystallite size <sup>b</sup> (nm)	22.0	22.4	18.0
Powder density ( $\text{g}/\text{cm}^3$ )	5.08	5.03	4.99
Relative density (%)	95.4	95.7	96.6
Lattice parameters ( $a$ ) (Å)	8.434	8.381	8.332
Combustion flame time (s)	7.0	12.0	11.0
Combustion flame temperature (°C)	673	703	622

<sup>a</sup> Calculated from specific superficial area.

<sup>b</sup> Calculated from Scherrer's formula.<sup>15</sup>

face area, particle size, crystallite size, powders density, lattice parameters, and flame combustion time and temperature) prepared by combustion reaction. The specific surface area (BET) and the nanoparticle size calculated from BET were  $37.9 \text{ m}^2/\text{g}$  and 36.0 nm;  $43.5 \text{ m}^2/\text{g}$  and 26.2 nm; and  $55.2 \text{ m}^2/\text{g}$  and 20.2 nm for the powders with  $x=0, 0.5$  and 1, respectively. Comparing these values with Scherrer's equation (22.0, 22.4 and 18.0 nm), it was observed that the values were close indicating the efficiency of the synthesis process. The densities of the powder were  $5.08 \text{ g}/\text{cm}^3$  (95.4% of the theoretical density),  $5.03 \text{ g}/\text{cm}^3$  (95.7% of the theoretical density), and  $4.99 \text{ g}/\text{cm}^3$  (96.6% of the theoretical density) for the powders with  $x=0, 0.5$  and 1, respectively. The results show that the increase of the  $\text{Ni}^{2+}$  concentration tends to produce powders with lowest combustion temperature, avoiding, this way, the pre-sintering and/or the growth of particles which leads to the formation of powders with the best nanocharacteristics.

We can observe that the increase of  $\text{Ni}^{2+}$  ions concentration caused a reduction of the value of the lattice parameter, " $a$ " of 1.2% when the value of the lattice parameter of the  $\text{ZnFe}_2\text{O}_4$  (8.434 Å) ferrite is compared with the value of the lattice parameter of the  $\text{NiFe}_2\text{O}_4$  (8.332 Å) ferrite. This can also be explained by the ionic radius difference between the  $\text{Ni}^{2+}$  and  $\text{Zn}^{2+}$  ions which is 6.7%.

Fig. 2 presents the size, morphology, and electron diffraction patterns of as-synthesized nickel ferrite particles observed by TEM micrograph.

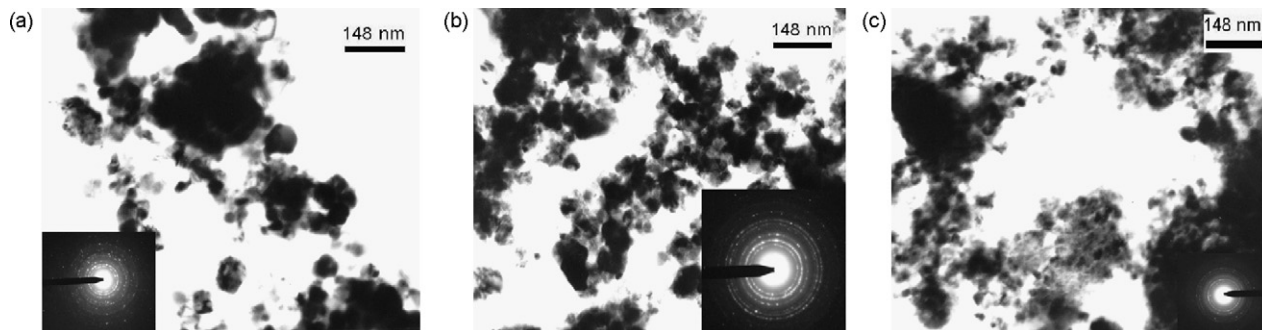


Fig. 2. TEM micrographs obtained for the compositions  $\text{Ni}_{1-x}\text{Zn}_x\text{Fe}_2\text{O}_4$ . (a)  $x=0$ , (b)  $x=0.5$  and (c)  $x=1$ .

Table 2

Pigments	$L^*$	$a^*$	$b^*$
$x=0$ (NF)	42.356	21.252	28.915
$x=0.5$ (NZF)	31.738	12.357	14.803
$x=1$ (ZF)	27.87	9.564	9.995

The electron diffraction clearly shows, in both cases, the rings which are characteristic of the nickel ferrite phase and also the rings corresponding to spacing of around 2.97 and 1.62 Å of the nickel ferrite. The selected area aperture used in this study was enough to reveal all the corresponding rings for the spinel structure. The TEM results showed that the particles did not have a narrow size distribution. Thus, it can be inferred that the nucleation occurred as a single event, and this resulted in a size distribution of nuclei. The particle size calculated by TEM micrograph in non-agglomerated regions was in the range of 18–29, 11–26, and 22–29 nm for the powders ZF, NZF, and NF, respectively. These results are in broad agreement with the results obtained by BET and Scherrer's equation. The particle size value obtained by the combustion reaction is in the range of the values calculated by TEM micrograph and reported by Chen<sup>2</sup> for NiFe<sub>2</sub>O<sub>4</sub> nanoparticles (5–30 nm) prepared by the sol–gel method.

Table 2 shows the data of the colorimetric coordinates  $L^*a^*b^*$  of Ni<sub>1-x</sub>Zn<sub>x</sub>Fe<sub>2</sub>O<sub>4</sub> ( $x=0$ ,  $x=0.5$ ,  $x=1$ ) pigments.

Table 2 shows the colorimetric coordinates in the plan  $a \times b$  for the pigments in agreement with what is illustrated in Fig. 3.

It can be observed a decrease in the  $L^*$ ,  $a^*$  and  $b^*$  parameters with the increase of the Ni<sup>2+</sup> concentration due to the tetrahedral coordination change (NC=4) for the octahedral coordination (NC=6) established by the substitution of Zn<sup>2+</sup> for Ni<sup>2+</sup> ions. The composition NF shows the smallest values of colorimetric parameters resulting in darker color than the composition ZF.

The diffuse reflectance spectra of the synthesized Ni<sub>1-x</sub>Zn<sub>x</sub>Fe<sub>2</sub>O<sub>4</sub> ( $x=0$ ,  $x=0.5$ ,  $x=1$ ) samples are shown in Fig. 4. The spectra for the pure NiFe<sub>2</sub>O<sub>4</sub> compound shows an absorbance band around 700 nm, which corresponds to the nickel ions in the octahedral sites. The absorbance band,

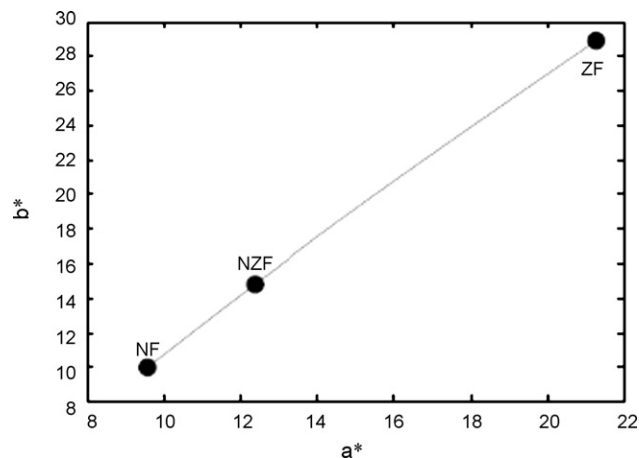


Fig. 3. Colorimetric parameters in the plan  $a \times b$  of the pigments synthesized by combustion reaction.

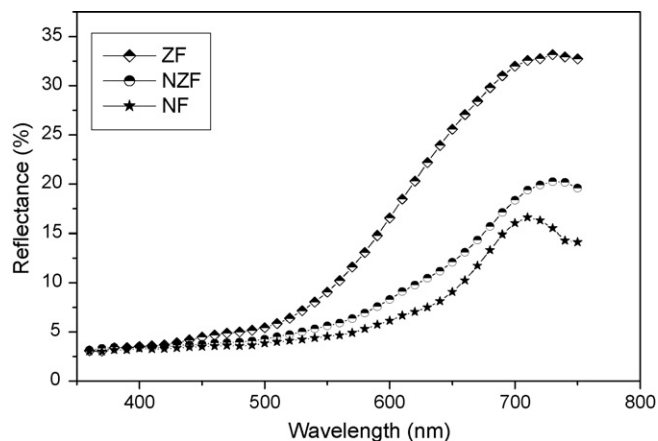


Fig. 4. Reflectance values diffused in function of the wavelength for the powders of the compositions Ni<sub>1-x</sub>Zn<sub>x</sub>Fe<sub>2</sub>O<sub>4</sub> ( $x=0$ ,  $x=0.5$ ,  $x=1$ ), resulting from the combustion reaction.

around 700 nm, shifts towards a higher wavelength region as the zinc concentration increases. This observation confirms that the Zn<sup>2+</sup> ion has a strong tetrahedral preference (NC=4). In addition, this variation causes modification in the color shade, varying from orange brown (ZF) to dark brown (NF), as a consequence of the structural change from the normal to the inverse spinel phase.

#### 4. Conclusion

The results obtained in the present work demonstrated that:

- The synthesis by combustion reaction was favorable for obtaining crystalline powders with nanosize particles ferrites type spinel.
- Increased concentrations of nickel (NF system) reduced the combustion flame temperature favoring the production of powders with nanometric characteristics, such as minute particle sizes and larger surface areas.
- The X-ray lines broadening and TEM confirmed the nature of the nanosize particle of the powder that was 11–29 nm.
- The substitution of the Ni<sup>2+</sup> for Zn<sup>2+</sup> ions causes structural change from the normal to the inverse spinel phase carrying the pigment color varying from orange brown to dark brown.

#### Acknowledgements

The authors would like to thank the Brazilian institutions CAPES and RENAMI-CNPq for their financial support for this research.

#### References

1. Peter, A. L., *Pigment Handbook*. John Wiley & Sons, New York, 1987.
2. Chen, N. S., Yang, X. J., Liu, E. S. and Huang, J. L., Reducing gas sensing properties of ferrite compounds MFe<sub>2</sub>O<sub>4</sub> (M=Cu, Zn, Cd and Mg). *Sens. Actuator B-Chem.*, 2000, **66**, 178–180.
3. Wang, L., Zhang, C., Li, S. and Wu, T., Studies on preparation and characterization of the spinel ferrite. *Chin. J. Inorg. Chem.*, 1996, **12**, 377–381.

4. Costa, A. C. F. M., Tortella, E., Morelli, M. R. and Kiminami, R. H. G. A., Effect of heating conditions during combustion synthesis on the characteristics of  $\text{Ni}_{0.5}\text{Zn}_{0.5}\text{Fe}_2\text{O}_4$  nanopowders. *J. Mater. Sci.*, 2002, **17**, 3569–3572.
5. Chen, Y. J., Liu, P. S. and Jin, Z. M., Studies of  $\text{La}_2\text{O}_3$  additive in Ni–Zn ferrite. *J. Mater. Sci. Lett.*, 1995, **14**, 998–1001.
6. Tsukimura, K., Sasaki, S. and Kimizuka, N., Cation distributions in nickel ferrites. *Jpn. J. Appl. Phys. Part 1. Regul. Pap. Short Notes Rev. Pap.*, 1997, **36**, 3609–3612.
7. Burghart, F. J., Potzel, W., Kalvius, G. M., Schreier, E., Grosse, G., Noakes, D. R., Schafer, W., Kockelmann, W., Campbell, S. J., Kaczmarek, W. A., Martin, A. and Krause, M. K., Magnetism of crystalline and nanostructured  $\text{ZnFe}_2\text{O}_4$ . *Physica B*, 2000, **289**, 286–290.
8. Tung, L. D., Kolesnichenko, V., Caruntu, G., Caruntu, D., Remond, Y., Golub, V. O., O'Connor, C. J. and Spinu, L., Annealing effects on the magnetic properties of nanocrystalline zinc ferrite. *Physica B*, 2002, **319**, 116–121.
9. Navrotsky, A. and Kleppa, O. J., The thermodynamics of cation distributions in simple spinels. *J. Inorg. Nucl. Chem.*, 1967, **29**, 2701–2714.
10. Lisboa-Filho, P. N., Vila, C., Petrucelli, G., Paiva-Santos, C. O., Gama, L., Ortiz, W. A. and Longo, E., *Physica B*, 2002, **320**, 249–252.
11. Xanthopoulou, G. G., Self-propagating SHS of inorganic pigments. *Am. Ceram. Soc. Bull.*, 1998, **77**, 87–96.
12. Eppler, R. A., Selecting ceramic pigments. *Am. Ceram. Soc. Bull.*, 1987, **66**, 1600–1607.
13. Bondioli, F., Ferrari, A. M., Leonelli, C. and Manfredini, T., Syntheses of  $\text{Fe}_2\text{O}_3$ /silica red inorganic inclusion pigments for ceramic applications. *Mater. Res. Bull.*, 1998, **33**, 723–729.
14. Costa, A. C. F. M., Morelli, M. R. and Kiminami, R. H. G. A., Combustion synthesis, sintering and magnetical properties of nanocrystalline Ni–Zn ferrites doped with samarium. *J. Mater. Sci.*, 2004, **39**, 1773–1778.
15. Kiminami, R. H. G. A., Combustion synthesis of nanopowder ceramic powder. *J. KONA*, 2001, **19**, 156–165.
16. Jain, S. R., Adiga, K. C. and Verneker, V. R. P., A new approach to thermochemical calculations of condensed fuel oxidizer mixtures. *Combust. Flame*, 1981, **40**, 71–79.
17. CIE, *Recommendations on Uniform Color Spaces, Color Difference Equations, Psychometrics Color Terms*. 1971 edition, supplement no. 2 of Cie Publ. no. 15 (e1-1.31). Bureau Central de la CIE, Paris, 1978.
18. Dean, J. A., In *Lange's Handbook of Chemistry*. 12th ed. McGraw-Hill, New York, 1979.
19. Costa, A. C. F. M., Morelli, M. R. and Kiminami, R. H. G. A., Microstructure and magnetic properties of  $\text{Ni}_{1-x}\text{Zn}_x\text{Fe}_2\text{O}_4$ . *J. Mater. Sci.*, 2007.
20. Cullity, B. D., *Elements of X-Ray Diffraction*, vol. 102. Addison-Wesley, California, 1978.
21. Callister Jr., W. D., In *Materials Science and Engineering An Introduction*. 3rd edn. John Wiley & Sons, Inc., New York, 1985.